Biology of Reproduction, 2023, **109(4)**, 520–532
https://doi.org/10.1093/biolre/ioad077
Advance access publication date 20 July 2023
Research Article

Rhox8 homeobox gene ablation leads to rete testis abnormality and male subfertility in mice†

Yeongseok Oh[1,2], Maho Kasu[1], Constence J. Bottoms[1], Jenna C. Douglas[1], Nikola Sekulovski[2], Kanako Hayashi[1,2] and James A. MacLean II[1,2,*]

[1]Center for Reproductive Biology, School of Molecular Biosciences, College of Veterinary Medicine, Washington State University, Pullman, Washington, USA
[2]Department of Physiology, Southern Illinois School of Medicine, Carbondale, IL, USA
***Correspondence:** Center for Reproductive Biology, School of Molecular Biosciences, College of Veterinary Medicine, Washington State University, Pullman, Washington 99164, USA. Tel: +15093352533; E-mail: james.maclean@wsu.edu

†**Grant Support**: This work was supported by NIH grant R01HD093802 (to JAM).

Abstract

The reproductive homeobox X-linked (*Rhox*) genes encode transcription factors that are expressed selectively in reproductive tissues including the testis, epididymis, ovary, and placenta. While many *Rhox* genes are expressed in germ cells in the mouse testis, only *Rhox8* is expressed exclusively in the Sertoli cells during embryonic and postnatal development, suggesting a possible role of *Rhox8* in embryonic gonad development. Previously, Sertoli cell–specific knockdown of RHOX8 resulted in male subfertility due to germ cell defects. However, this knockdown model was limited in examining the functions of *Rhox8* as RHOX8 knockdown occurred only postnatally, and there was still residual RHOX8 in the testis. In this study, we generated new *Rhox8* knockout (KO) mice using the CRISPR/Cas9 system. Sex determination and fetal testis development were apparently normal in mutant mice. Fertility analysis showed a low fecundity in *Rhox8* KO adult males, with disrupted spermatogenic cycles, increased germ cell apoptosis, and reduced sperm count and motility. Interestingly, *Rhox8* KO testes showed an increase in testis size with dilated seminiferous tubules and rete testis, which might be affected by efferent duct (ED) *Rhox8* ablation dysregulating the expression of metabolism and transport genes in the EDs. Taken together, the data presented in this study suggest that *Rhox8* in the Sertoli cells is not essential for sex determination and embryonic testis differentiation but has an important role in complete spermatogenesis and optimal male fertility.

Summary Sentence

Rhox8 knockout results in male subfertility together with a disrupted spermatogenic cycle, increased germ cell apoptosis, and reduced sperm count and motility, suggesting that *Rhox8* has an important role for optimal male fertility.

Graphical Abstract

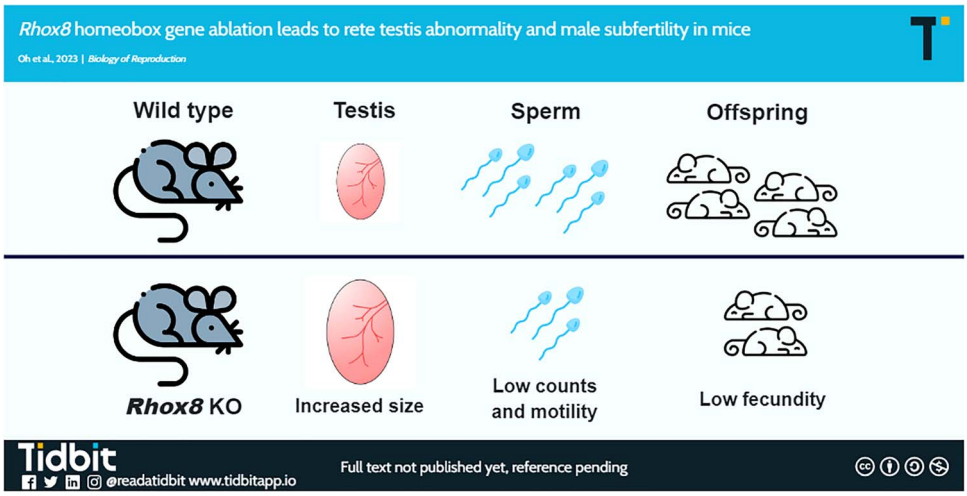

Keywords: male fertility, spermatogenesis, Sertoli cells, rete testis, efferent ducts, reproductive homeobox X-linked gene, *Rhox8*

Received: February 23, 2023. **Revised:** July 10, 2023. **Accepted:** July 15, 2023

Introduction

Spermatogenesis is the process that produces male haploid germ cells (spermatozoa) from diploid spermatogonial stem cells in the seminiferous tubules (STs) of the testis. In the testis, the Sertoli cells, as the somatic constituents of the seminiferous epithelium, are directly associated with all types of germ cells including spermatogonia, spermatocytes, spermatids, and spermatozoa and are primarily committed to sustaining spermatogenesis as they nourish the developing germ cells [1]. In the Sertoli cells, many transcription factors have been identified, including homeobox, SRY-related HMG-box, zinc-finger, heat-shock, and cAMP-response family members, and their essential roles in controlling testis development and spermatogenesis have been studied, particularly using knockout (KO) mouse models [2, 3]. While many transcription factors have been known to be expressed in Sertoli cells, their roles in testis development as well as in spermatogenesis remain to be investigated. Particularly, the global ablation of homeobox factors expressed in non-gonadal tissues often results in developmental errors, which result in embryonic lethality.

Homeobox genes encode transcription factors containing a homeodomain that consists of ~60 amino acid DNA binding motif [4]. Homeodomain proteins regulate gene expression and cell differentiation during embryonic development including body-axis formation, organogenesis, and limb development [5, 6]. Thus, mutations in the homeobox genes often lead to developmental disorders [5, 6]. Rodent genomes contain ~200 homeobox genes, 25% of which are known to be expressed in the testis [7, 8]. However, an evident function of the majority has not been identified. Among the homeobox genes, the reproductive homeobox X-linked (*Rhox*) genes are known to be selectively expressed in both male and female reproductive tissues including the testis, epididymis, ovary, and placenta. To date, 33 *Rhox* genes have been identified in the mouse genome, and many *Rhox* genes are expressed in germ cells [7, 8]. However, only *Rhox5* and *Rhox8* are expressed in Sertoli cells [9, 10], suggesting that these genes regulate the expression of Sertoli cell genes critical for male germ cell development. *Rhox5*, the founding member of the *Rhox* cluster, is regulated by androgen, and its ablation results in male subfertility together with increased germ cell apoptosis and compromised sperm motility [9]. RHOX8 in vivo knockdown in Sertoli cells using a tissue-specific RNAi approach results in reduced spermatogenic output, increased germ cell apoptosis, and decreased sperm motility, leading to impaired male fertility, which is similar to phenotypes of the *Rhox5* null male mice [10]. In the fetus, *Rhox8* is the only member of the *Rhox* gene family that is expressed in the Sertoli cells of the embryonic gonads, while *Rhox5* is expressed in the embryonic germ cells [11], suggesting a unique role of *Rhox8* in embryonic Sertoli cell specification and function. However, in the RHOX8 knockdown model used in the previous study, RHOX8 expression was not initially targeted until postnatal day 5 when the androgen-regulated, Sertoli cell–specific *Rhox5* promoter used to drive the *Rhox8*-siRNA transgene is first active. Subsequently, significant RHOX8 knockdown was not achieved until postnatal day 18 [10], creating a limitation of the RHOX8 knockdown model to study the role of *Rhox8* in the embryonic Sertoli cell function and the first wave of spermatogenesis. In addition, some RHOX8 functionality may have remained after siRNA activation due to the actions of the residual RHOX8 protein. Therefore, a new strategy was required to overcome these obstacles.

In the present study, in an effort to elucidate the function of *Rhox8* in the testis, a *Rhox8* KO mouse model was created through the clustered regularly interspaced short palindromic repeats/CRISPR associated protein 9 (CRISPR/Cas9) technology [12], and its phenotypes were investigated. We show that *Rhox8* KO male mice are subfertile together with a disturbed spermatogenic cycle, increased germ cell apoptosis, and reduced sperm concentration and motility, suggesting an important role of *Rhox8* in germ cell development and function.

Materials and methods

Experimental animals and generation of *Rhox8* knockout mice

All animal experiments were performed in accordance with the relevant National Institutes of Health guidelines and in compliance with the Southern Illinois University Carbondale and the Washington State University Institutional Animal Care and Use Committees. To produce *Rhox8* mutant mice, C57BL/6 J mouse embryos at the one-cell stage and CRISPR/Cas9 reagents were electroporated by the Genome Editing and Animal Models Core at the University of Wisconsin Biotechnology Center. The guide RNA sequence used in the gene editing is 5′-GACGACTGGGTGACTTCTTG-3′. The embryos were implanted into pseudopregnant recipients (B6D2F1 background). A single founder carrying 2-bp (TT) insertion was identified and backcrossed to C57BL/6 J. Wild-type (*Rhox8*$^{+/Y}$) and *Rhox8* KO (*Rhox8*$^{-/Y}$) male embryos or mice were generated by crossing wild-type (WT) or *Rhox8* KO males with *Rhox8* heterozygous (*Rhox8*$^{+/-}$) females. Genotyping was done using genomic DNA extracted from tail snips. PCR was performed using a primer set: 5′-AAGTGGGCCAGGCCAGAAGAG-3′ (forward) and 5′-AAGGAAGGGCTGCAGGCAGAG-3′ (reverse). Then, the amplified DNA (284 bp for WTs; 286 bp for mutants) was digested with a restriction enzyme, *Bpu*EI. The fragments of 116 and 168 bp were detected in the WT, or the intact DNA of 286 bp was detected in *Rhox8* KO.

To collect embryonic testes, the embryos on embryonic days 12.5 (E12.5), E13.5, E14.5, and E15.5 were obtained from pregnant mice, and then, the gonads were dissected from the embryos. The morning of an observed mating plug was defined as E0.5. The embryos were sexed by morphological assessment at the time of collection and later confirmed by PCR for *Sry* gene using a primer set: 5′-CATCGGAGGGCTAAAGTGTC-3′ (forward) and 5′-TTGGAGTACAGGTGTGCAGC-3′ (reverse). The obtained testes were subjected to quantitative real-time reverse transcription polymerase chain reaction (RT-PCR) or immunofluorescence staining. To test fertility of the mice, WT and *Rhox8* KO male mice at 2 months of age were housed with two WT C57BL/6 female mice (*Rhox8*$^{+/+}$) at 2 months of age for 5 days or 8 weeks. The number of litters and pups were systematically recorded. To analyze postnatal testes, the tissues were obtained from the WT and *Rhox8* KO mice at 12 days (P12), 30 days (P30), 2 months (2mo), and 3 months (3mo) of age and subjected to further experiments.

Immunohistochemistry

Immunohistochemistry was performed as described previously with some modifications [13]. Tissues were fixed in Bouin's solution and then embedded in paraffin. Sections (5 μm) were mounted on glass slides, deparaffinized, and rehydrated. Antigen retrieval was performed using 10 mM citrate buffer at 110°C for 10 min. The slides were incubated in 1% H_2O_2 in methanol to block endogenous peroxidase activity. Then, the immunostaining was performed using a VECTASTAIN Elite ABC Kit (PK-6101, Vector Laboratories). The primary antibodies for RHOX8 (1:2000 dilution, NBP2-23671, Novus Biologicals) and SOX9 (1:1000 dilution, AB5535, Millipore) were applied overnight at 4°C. The signal was developed using a 3,3′-diaminobenzidine (DAB) substrate kit (SK-4105, Vector Laboratories); the nuclei were stained using hematoxylin. From the SOX9-stained sections, SOX9-positive cells and the total STs were counted, and the numbers of Sertoli cells per ST were calculated. For immunofluorescence staining, the tissues were fixed in 4% paraformaldehyde in PBS and then embedded in paraffin. Sections (5 μm) were mounted on glass slides, deparaffinized, and rehydrated. Antigen retrieval was performed using 10 mM citrate buffer at 110°C for 10 min. The slides were blocked with 5% donkey serum for 30 min and then incubated in Alexa Fluor 555-conjugated SOX9 antibody (AB5535-AF555, Millipore) diluted 1:100 in 1% donkey serum at room temperature for 1 h. The nuclei were stained using DAPI.

Sperm analysis

Sperm analysis was performed as described previously with some modifications [10]. The cauda epididymis was dissected from WT and *Rhox8* KO male mice, cut one time, placed in 500 μl EmbryoMax M2 medium (Millipore) warmed to 37°C, and incubated for 10 min. After the incubation, 8 μl of the sperm suspension was placed in the center of a Cell-Vu sperm counting chamber. And then, motile and non-motile sperm were counted under a dark-field microscope to determine sperm concentration and motility. For more sophisticated and automated analysis, sperm samples were incubated at 37°C for 15 min and analyzed using computer-assisted sperm analysis (CASA) (SCA CASA system; Fertility Technology Resources, Inc.) following the manufacturer's instructions as previously described [14, 15].

Detection of DNA fragmentation in situ

Paraffin sections (5 μm thick) of testes isolated from WT and *Rhox8* KO mice at 2–3 months of age were subjected to detection of DNA fragmentation. The DNA fragmentation in sections was identified by TUNEL (terminal deoxynucleotidyl transferase dUTP nick end labeling) using an in situ cell death detection kit (Roche, Mannheim, Germany). In brief, sections were dewaxed, rehydrated, and incubated with permeabilization solution (0.1% Triton X-100, 0.1% sodium citrate) for 8 min. After washing in PBS, sections were incubated with TUNEL reaction mixture (label and enzyme solution) for 60 min at 37°C in a humidified atmosphere in the dark. The sections were counterstained with DAPI. TUNEL-positive STs and cells were counted, and the percentages of TUNEL-positive STs and the numbers of TUNEL-positive cells per ST were calculated as described previously [9, 10, 16].

Quantitative reverse transcription polymerase chain reaction

Total RNA was isolated from the testes, efferent ducts (EDs), and epididymides using a TRIzol reagent (Invitrogen), and then RT was performed using a High-Capacity cDNA Reverse Transcription Kit (Applied Biosystems). Real-time PCR was performed using PowerUp SYBR Green Master Mix (Applied Biosystems) in a StepOnePlus Real-time PCR System (Applied Biosystems). Real-time PCR was performed using the following protocol: 2 min at 95°C, 40–45 cycles of denaturation (15 s at 95°C) and annealing/extension (1 min at 60°C), and a final step of melting curve analysis. As an internal control, *Rpl19* was used. The relative levels of mRNA were calculated using the $2^{-\Delta\Delta Ct}$ method. The primers for gene amplification have been previously reported [10, 13, 17–21] or are listed in Supplementary Table S1.

Statistical analysis

Data were analyzed by the Student *t*-test for the comparison between WT and *Rhox8* KO at the same time point or by the chi-square (χ^2) test for the estimation of sex or genotype distribution using Prism (GraphPad) or Excel software (Microsoft Office). Significance was accepted when the *P*-value was smaller than 0.05.

Results

Generation of *Rhox8* knockout mice

To elucidate the function of *Rhox8*, we used CRISPR/Cas9 technology to ablate *Rhox8* in the mouse. The mutant mice were generated by introducing a guide RNA/Cas9 expression vector into mouse embryos. As a result, a mutant line carrying a 2-bp (TT) insertion was established. In this mouse line, a frame shift mutation was induced, which leads to premature termination of translation at a new termination codon (TGA) (Figure 1A). For the genotyping, genomic DNA was extracted from tail snips, PCR was performed using a primer set, and then, the amplified DNA was digested with a restriction enzyme, *Bpu*EI. The fragments of 116 and 168 bp were detected in the WT allele, or the intact DNA of 286 bp was detected in the *Rhox8* KO allele (Figure 1B). To validate the absence of RHOX8 protein in the *Rhox8* KO mice, immunohistochemical analysis for RHOX8 was performed using mouse testes at P12 when the *Rhox8* expression is relatively the highest temporally in total testis after birth as well as when the Sertoli cells make up approximately half of the cells within STs [10, 22]. The RHOX8 protein was not detectable in *Rhox8* KO testis, while RHOX8 was localized in the nuclei of all the Sertoli cells of WT testis (Figure 1C), indicating a complete *Rhox8*-null mutation in the mutant mice.

Effect of *Rhox8* ablation on the embryonic testis development

Rhox8 is expressed in the Sertoli cells of embryonic gonads [11], and RHOX8 putatively regulated *Sox9* postnatally [10], suggesting a possibility that *Rhox8* participates in the sex determination or sex maintenance during embryo gonad development if it regulates *Sox9* in the embryo. To begin to determine the involvement of *Rhox8* in sex determination, we observed the sex distribution of the pups produced from breeding pairs. For the breeding, each WT or *Rhox8* KO male

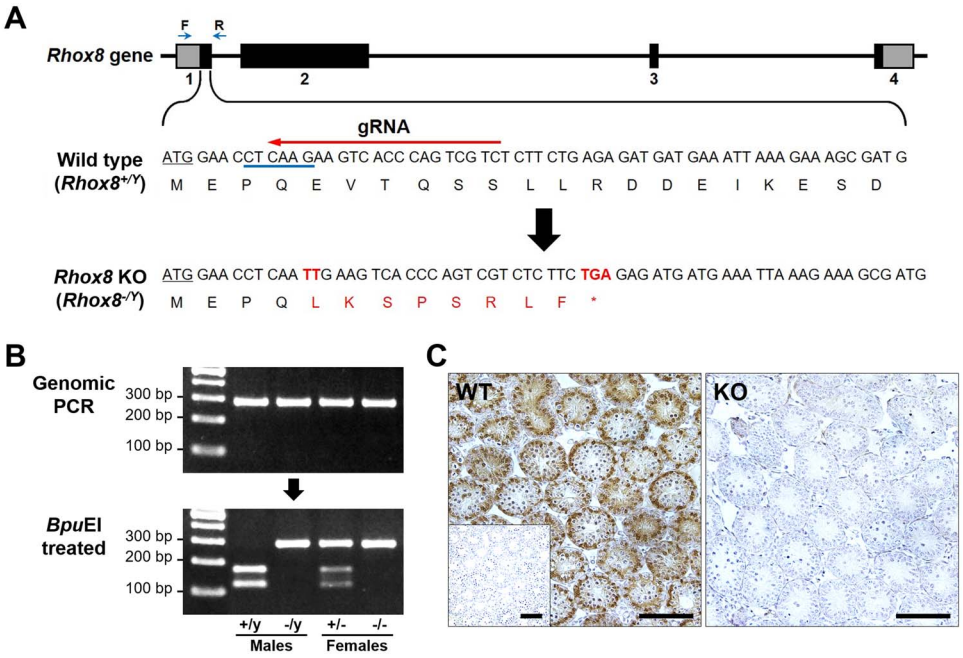

Figure 1. Generation of *Rhox8* KO mice. (A) Schematic drawing for *Rhox8* gene editing. The *Rhox8* KO mice were generated using CRISPR/Cas9 technology. The *Rhox8* gene consists of four exons. The coding sequences of exon 1 and their corresponding amino acids are presented below the *Rhox8* gene structure. A guide RNA (gRNA) applied in the gene editing is presented above WT DNA sequence. The blue-lined sequence is a restriction site that is recognized by a restriction enzyme, *Bpu*EI. In the mutant, a frame shift was induced by an insertion of two bases (TT), resulting in premature termination of translation at a new stop codon (TGA). F and R, forward and reverse PCR primers used in genotyping PCR. (B) Genomic PCR and restriction enzyme treatment for genotyping. After *Bpu*EI treatment, the WT male shows two fragments (116 and 168 bp), and the mutant male shows the intact DNA (286 bp). A heterozygous female shows three bands (116, 168, and 286 bp). (C) Immunohistochemical analysis for RHOX8 in the testes at postnatal day 12. The RHOX8 protein is localized to Sertoli cells in the WT, whereas it is not detectable in the *Rhox8* KO. Inset presents a negative control in which preimmune serum was applied. Scale bars, 100 μm.

Table 1. Distribution of sexes and genotypes in the pups produced from breeders

Mating		No. of litters	No. of pups				Genotype of pups					
Male	Female		Total	♂	♀	*P*-value[a]	+/y	−/y	+/+	+/−	−/−	*P*-value[b]
Rhox8$^{+/Y}$	*Rhox8*$^{+/-}$	25	221	117	104	0.9431	59	58	46	58	0	0.7216
Rhox8$^{-/Y}$	*Rhox8*$^{+/-}$	22	191	98	93	0.9979	51	47	0	47	46	0.9810

[a]In both mating groups, no significant differences in the observed sex distribution of the pups were observed by χ^2-test. [b]In both mating groups, no significant differences in the observed genotype distribution of the pups were observed by χ^2-test.

was crossed with *Rhox8* heterozygous females. The neonates were sexed based on the external genitalia at first. In both mating groups (*Rhox8*$^{+/Y}$ male and *Rhox8*$^{+/-}$ female pairs and *Rhox8*$^{-/Y}$ male and *Rhox8*$^{+/-}$ female pairs), there were no significant differences between the numbers of males and females in the litters from any KO line (Table 1). After the initial sexing, from six independent litters per mating group, the sexes were validated by PCR for the *Sry* gene, and we could not find any sex reversal in all the tested litters (data not shown), indicating that *Rhox8* is not necessary for sex determination. The distribution of the genotypes from the litters was normal in both mating groups (Table 1), suggesting Mendelian inheritance of the mutant allele and no significant embryonic loss of mutant mice.

To determine whether *Rhox8* deficiency affects the development of embryonic testis, the testes were isolated from WT and *Rhox8* KO embryos at E12.5–E15.5 and were analyzed (Figure 2). We did not find a difference in the embryonic testis morphology between WT and *Rhox8* KO (Figure 2A). To identify *Rhox8*-regulated genes in the embryonic testis as well as to determine whether *Rhox8* is involved in embryonic testis development, we examined the temporal expression of the key genes essential for sex determination and gonad development in the embryonic testes from E12.5 to E15.5 (Figure 2B). At first, to examine the expression of *Rhox8* mRNA in *Rhox8* KO testes, quantitative RT-PCR was performed using a primer set containing a forward primer spanning the target region for gene editing. The *Rhox8* mRNA was barely detectable in *Rhox8* KO testes from E12.5 to E15.5. The expressions of *Sox9*, *Fgf9*, *Fgfr2*, *Ptgds*, *Amh*, and *Wnt4* mRNA were not significantly altered by *Rhox8* ablation from E12.5 to E15.5. Among them, in particular, the *Wnt4* mRNA level in *Rhox8* KO testes at E12.5 was increased by 1.63-fold compared to that in WT testes, although the difference is not statistically significant ($n = 4$; $P = 0.1202$). We analyzed a panel of germ cell–specific markers, *Pou5f1* (*Oct4*) and *Ddx4*, and found that their mRNA expression levels in *Rhox8* KO testes were significantly lower than those in the WT only at E13.5 ($P = 0.0147$ and 0.0332 for *Pou5f1* and *Ddx4* expression, respectively), indicative of a partial or transitory perturbation

Table 2. Effect of *Rhox8* ablation on male fertility

Mice	No. of pairs	No. of litters	Litter freq.[a]	Mean litter size[a]	No. of pups			
					Total	♂	♀	*P*-value[b]
5-day timed mating								
Rhox8$^{+/Y}$	21	20	0.95 ± 0.05	8.9 ± 0.3	178	94	84	0.4535
Rhox8$^{-/Y}$	20	11	0.55 ± 0.11**	9.1 ± 0.6	100	51	49	0.8415
8-week continuous mating								
Rhox8$^{+/Y}$	10	20	2.00 ± 0.00	9.0 ± 0.3	179	93	86	0.6008
Rhox8$^{-/Y}$	10	14	1.40 ± 0.23*	8.6 ± 0.7	120	59	61	0.8551

[a]Values are presented as mean ± SEM. *, $P < 0.05$; **, $P < 0.01$ versus Rhox8$^{+/y}$ by Student *t*-test. [b]No significant differences in the observed sex distribution of the pups were observed by χ^2-test.

of embryonic gonad development, which might be caused by *Rhox8* ablation. To confirm the normal expression of SOX9 protein in the *Rhox8* KO embryonic testes, immunofluorescence staining of SOX9 was performed using testes at E12.5–E15.5 (Figure 2C). There were no significant differences of SOX9 immunoreactivity between WT and *Rhox8* KO testes, which is consistent with the expression of *Sox9* mRNA.

Subfertility of *Rhox8* knockout male mice

To determine the reproductive fitness of *Rhox8* KO males, a fertility test was performed as each male mouse was paired with a WT female mouse (Table 2). In 5-day timed mating experiments in which 21 (for WT males) or 20 (for *Rhox8* KO males) pairs were observed, *Rhox8* KO mice produced 11 litters, while WTs produced 20 litters, indicating that the litter frequency was significantly reduced by *Rhox8* ablation (the average values were 0.95 and 0.55 for WT and *Rhox8* KO, respectively). When pairs were monitored for 8 weeks, the *Rhox8* KO males also showed significantly lower litter frequency than WT males (the average values were 2.00 and 1.40 for WT and *Rhox8* KO, respectively; $n = 10$ pairs each). Although *Rhox8* KO males showed low litter frequency, their litter size was not significantly different from those in WTs (the average values in the 5-day timed matings were 8.9 and 9.1 for WT and *Rhox8* KO, respectively, and 9.0 and 8.6 in the 8-week continuous matings). In addition, the numbers of males and females were counted. There were no significant differences in the sex ratio of the pups, which is consistent with our prior observation from breeding pairs (Table 1). During these fertility tests, the virginal plugs generated by males were checked every morning for 5 days. There was no significant difference between WT and *Rhox8* KO (17/21 matings in wild type and 17/20 matings in *Rhox8* KO; $P = 0.7385$), indicating a normal mating behavior of *Rhox8* KO males.

Germ cell defects in *Rhox8* KO male mice

Because male fecundity could be affected by sperm function, we examined sperm concentration and motility extracted from cauda epididymides of adult WT and *Rhox8* KO male mice. Manual counting of the caudal sperms showed that sperm count was significantly reduced to 63.5% of the WT sperms by *Rhox8* ablation ($P = 0.0039$), and sperm motility was also significantly reduced in the *Rhox8* KO, assessed to be 81.8% of the WT ($P = 0.0006$) (Figure 3A). These decreased sperm concentration and motility were confirmed by CASA ($P = 0.0001$ and 0.0005 for sperm count and motility, respectively; Figure 3B). These results indicate that sperm defect may be a factor causing the low fecundity in *Rhox8* KO males. Based on our previous studies in which the low spermatogenic output of mutants was attributed to increased germ cell apoptosis [9, 10, 16, 23], we performed TUNEL assay using testis cross sections obtained from adult WT and *Rhox8* KO mice, and TUNEL-positive STs and cells were counted. In *Rhox8* KO mice, the number of TUNEL-positive cells per ST ($P = 0.0444$) as well as the percentage of TUNEL-positive tubules ($P = 0.0357$) was significantly increased (Figure 3C). Most of the TUNEL-positive cells were likely germ cells (mainly spermatocytes), based on their position within STs. Therefore, these results indicate that the reduced sperm concentration in *Rhox8* KO arose due to the increased apoptotic germ cells.

Spermatogenesis, as a complex biological process of germ cell transformation, is strictly orchestrated with seminiferous epithelium periodically cycling diverse stages defined by the combination of germ cell types that can be found within a cross section of an ST [24]. In the mouse, the spermatogenic cycle of the seminiferous epithelium is divided into 12 stages [25]. To determine whether spermatogenesis was affected in *Rhox8* KO mice, we examined the distribution of spermatogenic stages (Figure 3D), as described previously [10, 24, 26]. In *Rhox8* KO, the proportion of the STs at stages I–VI was significantly increased, while fewer STs at stage VII and VIII were observed (Figure 3E). There were no significant differences between WT and *Rhox8* KO at stage IX and afterward. This result indicates a partial inhibition of the spermatogenic cycle in *Rhox8* KO males, particularly in the early stage to stage VII transition.

Physical and histological changes in *Rhox8* knockout male mice

As the loss of *Rhox8* resulted in spermatogenic defects including altered spermatogenic cycle, increased germ cell apoptosis, and reduced spermatogenic output in the males, we expected that physical and histological changes would accompany the phenotypes of *Rhox8* KO. The male mice at ages P12, P30, 2mo, and 3mo were used to assess body and testis weight. There were no differences in the body weight between WT and *Rhox8* KO in all age groups tested (Figure 4A). However, testis weights and the ratio of the testis to body weight in *Rhox8* KO mice were higher than those in WT from P30 onward with an increased testis size (Figure 4B–D). In addition, the ST diameter was slightly, but significantly, higher in *Rhox8* KO testes at 2mo–3mo (Figure 4E). The number of Sertoli cells per ST was not affected by *Rhox8* ablation (Figure 4F), which was assessed by counting Sertoli cell nuclei after immunostaining of SOX9, a Sertoli cell marker. The

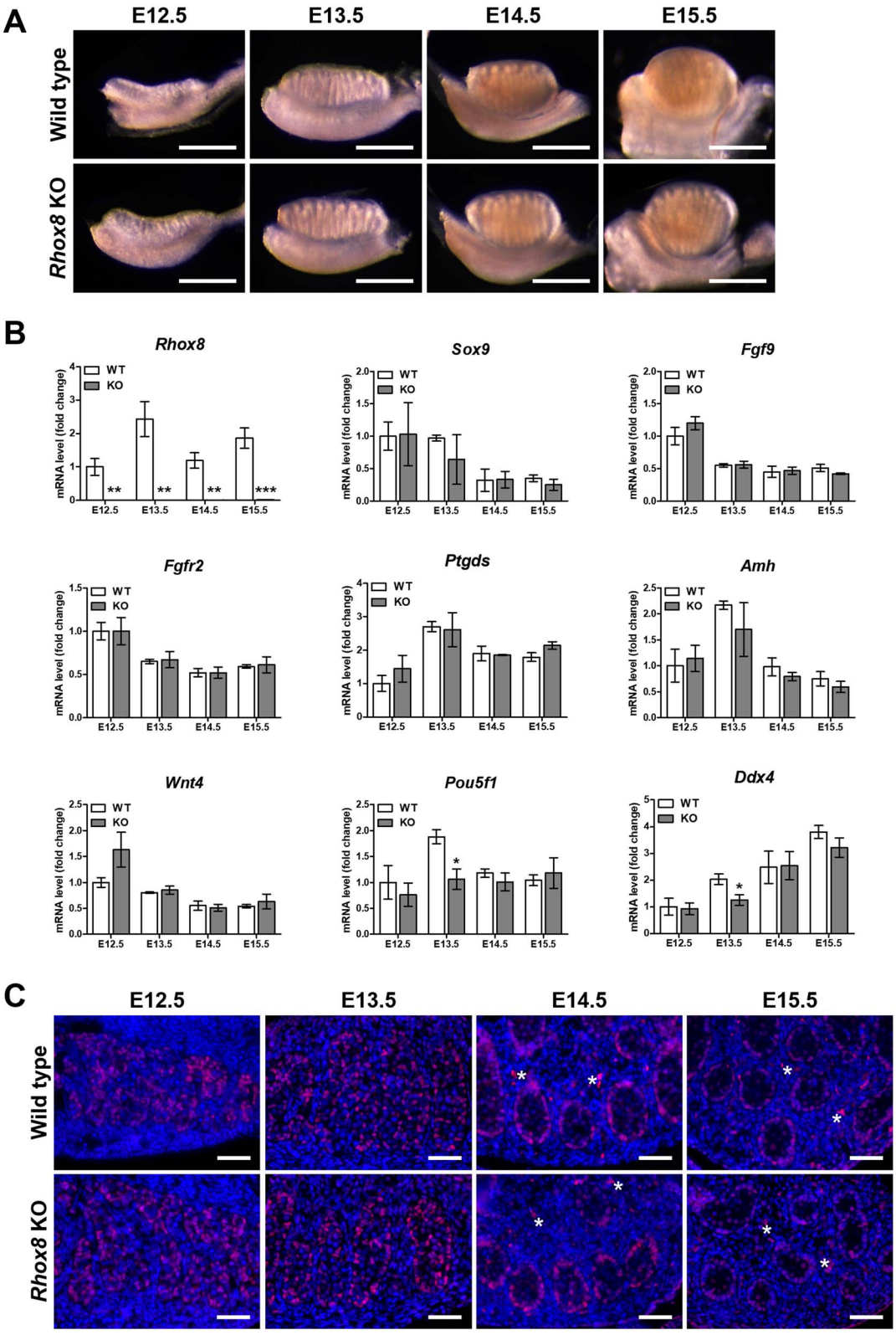

Figure 2. Normal development of embryonic testis in *Rhox8* KO mice. (A) Representative images of testes isolated from WT and *Rhox8* KO embryos at embryonic day 12.5 (E12.5), E13.5, E14.5, and E15.5. Scale bars, 500 μm. (B) Quantitative RT-PCR analysis of WT and *Rhox8* KO testes at E12.5, E13.5, E14.5, and E15.5. As an internal control, *Rpl19* mRNA was used. The data are presented as the means ± SEM ($n = 4$). $^{*}P < 0.05$, $^{**}P < 0.01$, $^{***}P < 0.001$. (C) Immunofluorescence staining for SOX9 (red) in WT and Rhox8 KO testes at E12.5, E13.5, E14.5, and E15.5. The nuclei (blue) were stained using DAPI. Asterisks indicate non-specific autofluorescence in the interstitium. Scale bars, 50 μm.

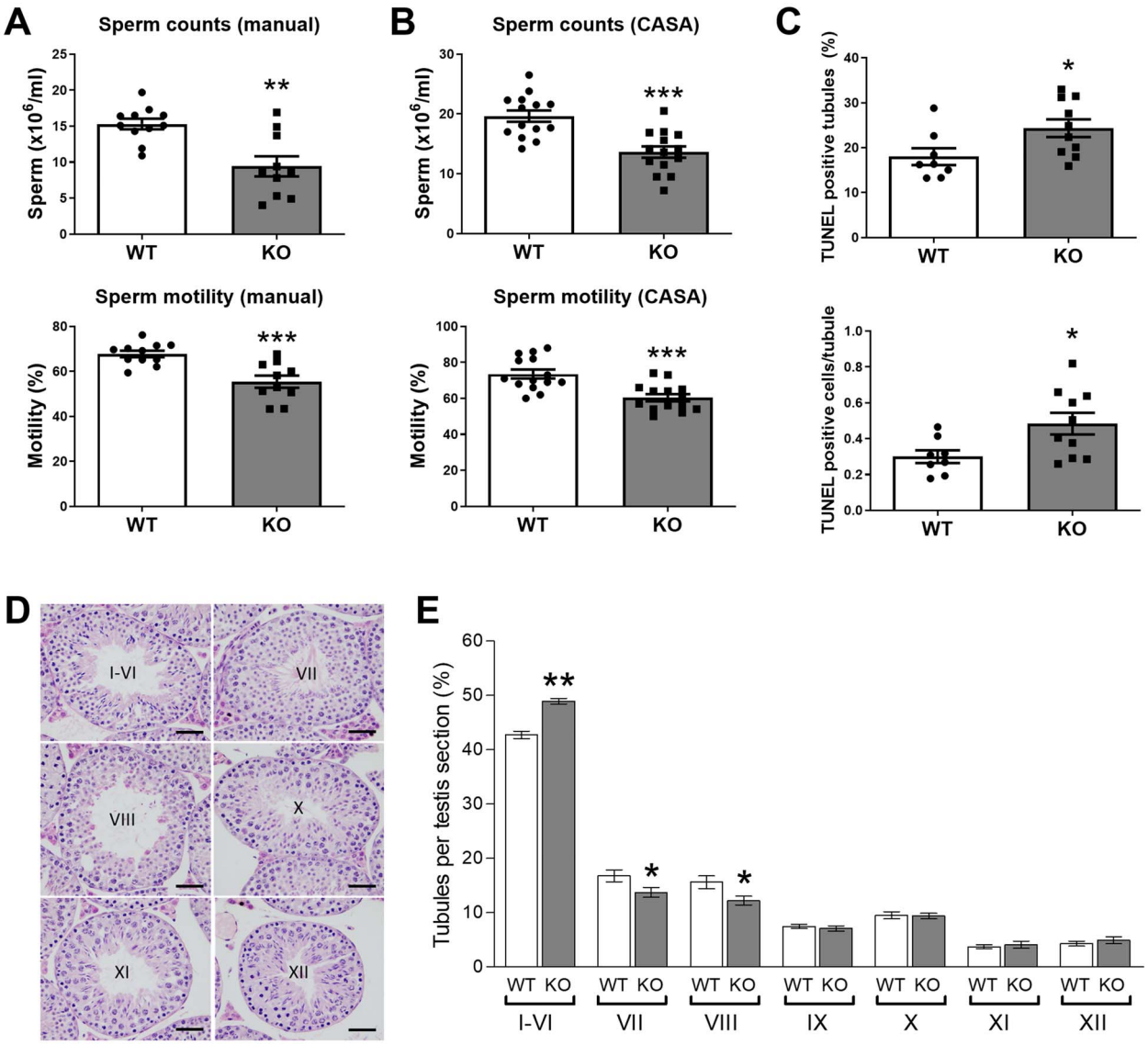

Figure 3. Analysis of germ cell defects in *Rhox8* KO mice. (A) Cauda epididymal sperm counts and motility were manually determined in WT ($n = 11$) and *Rhox8* KO ($n = 10$) mice under a dark-field microscope. (B) Using computer-assisted sperm analysis (CASA), the sperm counts and motility were analyzed ($n = 14$ each). (C) TUNEL assay of WT and *Rhox8* KO mouse testes. TUNEL-positive STs and cells were counted, and the percentages of TUNEL-positive STs and the numbers of TUNEL-positive cells per ST were calculated ($n = 8$ for WT; $n = 10$ for KO). The data are presented as the means ± SEM. $^{*}P < 0.05$, $^{**}P < 0.01$, $^{***}P < 0.001$. (D) Testis sections from the mice were stained with hematoxylin and eosin. And then, the stages of spermatogenic cycle were identified in each ST. Scale bars, 50 μm. (E) Comparison of the relative proportions of the spermatogenic stages in WT and *Rhox8* KO mice. The data are presented as the means ± SEM ($n = 10$) . $^{*}P < 0.05$, $^{**}P < 0.01$.

increase in testis weight and ST diameter of *Rhox8* KO was unexpected as these findings were opposite results from our previous study in which RHOX8 knockdown in Sertoli cells resulted in decreased testis weight and tubule diameter [10]. Intriguingly, further histological analysis showed a dilated rete testis (RT) in *Rhox8* KO testis (Figure 4G), which has not been observed in the RHOX8 knockdown mice [10].

Analysis of transition region and efferent ducts in *Rhox8* knockout mice

The transition region (TR), as an area that forms the junction between STs, is composed of modified Sertoli cells and a low population of germ cells, and the modified Sertoli cells form a valve-like structure to prevent fluid reflux from the RT [27]. The EDs connect the RT with the initial section of the epididymis and has a function of absorption of water from the fluid produced by the testis [28]. Therefore, the TR and EDs have an important role to maintain the environment of the STs and RT and hence might be responsible for testis size. To address the physiological issue of the increased testis size with the dilated RT in *Rhox8* KO mice, we examined the expression of *Rhox8* in the TR and EDs, the morphology of the modified Sertoli cells in the TR, and the expression of functional genes in the EDs. Immunohistochemical analysis showed that RHOX8 protein is expressed in the modified Sertoli cells in the TR and a few epithelial cells in the RT of WT mouse, whereas it is not detectable in *Rhox8* KO (Figure 5A). In the EDs, the RHOX8 protein is localized to ciliated cells in WT (Figure 5B). To determine whether loss of *Rhox8* affects the function of the TR, histological analysis was performed in the TR. Both WT and *Rhox8* KO showed normal Sertoli cells of valve-like structure (Figure 5C). A previous study revealed

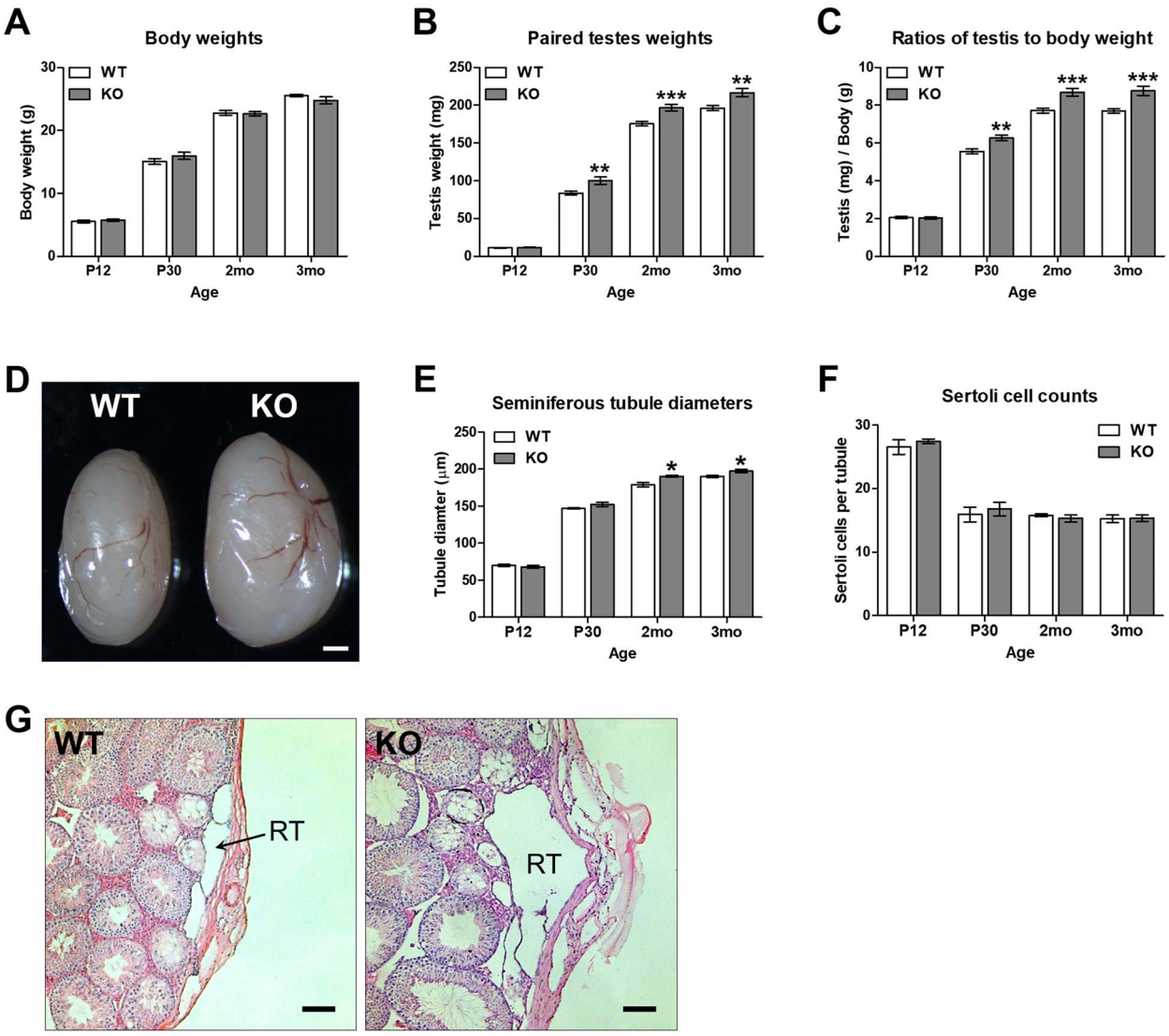

Figure 4. Physical and histological analysis in WT and *Rhox8* KO mice. The male mice at 12 days (P12; $n = 10$ and 11 for WT and KO, respectively), 30 days (P30; $n = 8$ and 6), 2 months (2mo; $n = 10$ and 8), and 3 months (3mo; $n = 9$ and 8) of age were subjected to measure body weight (A) and testis weight (B). (C) The ratio of testis to body weight. (D) Representative image of testes isolated from WT and *Rhox8* KO mice at 2mo. Scale bar, 1 mm. (E) The diameters of the seminiferous tubules were measured using ImageJ program after hematoxylin and eosin staining of testis sections ($n = 6$). (F) The numbers of Sertoli cells were counted after immunostaining for SOX9 on testis sections ($n = 6$). The data are presented as the means ± SEM. $^{*}P < 0.05$, $^{**}P < 0.01$, $^{***}P < 0.001$. (G) Hematoxylin and eosin–stained testis sections. The dilated RT were observed in *Rhox8* KO mice. Scale bars, 100 μm.

that dysregulation of Notch-FGF signaling contributes to a dilated RT in mice [21]. Hence, we investigated the expression of Notch target genes, *Hes1* and *Hey1*, as well as *Fgf4* in the testes. There were no significant differences in the expression of these genes (Figure 5D). When we examined the expression of *Rhox8* mRNA in the excurrent ducts including the EDs and caput, corpus, and cauda epididymis, the *Rhox8* expression is the highest in the EDs (Figure 5E), suggesting a possible role of *Rhox8* in the function of EDs. It has been known that *Esr1* ablation in the EDs cause an inhibition of fluid reabsorption from the lumen, which is related to increased testis size with dilated STs and RT [29, 30], suggesting a possible interaction between the *Rhox8* and *Esr1* genes. To determine a possibility of the involvement of *Rhox8* in the ESR1 pathway, we examined the expression of *Esr1* and *Esr1*-regulated genes (*Aqp1*, *Aqp9*, *Car2*, *Car14*, *Slc4a4*, and *Slc9a3* which are downregulated in *Esr1* KO; *Cftr*, *e*, and *Slc26a3*, which are upregulated in *Esr1* KO) [31]. The expression of *Car14*, *Slc9a3*, *Cftr*, and *Slc9a1* was significantly reduced in *Rhox8* KO EDs; meanwhile, there were not significant changes in the expression of the other genes in the *Rhox8* KO (Figure 5F), which does not coincide with that in *Esr1* KO, suggesting that *Rhox8* regulates functional genes in the EDs through another mechanism than the ESR1 pathway.

Expression of Sertoli cell–specific genes in *Rhox8* knockout testes

In our previous study, in P18 and P30 testes, RHOX8 knockdown downregulated the expression of two genes, *Sox8* and *Sox9* [10], which are crucial for Sertoli cell development and function [32]. However, in this study, the expressions of *Sox8* and *Sox9* mRNA were not altered by *Rhox8* ablation in the testes from P12 to 3mo (Figure 6), indicative of different gene regulation between the RHOX8 knockdown and *Rhox8* KO models. The mRNA expression of two other Sertoli cell

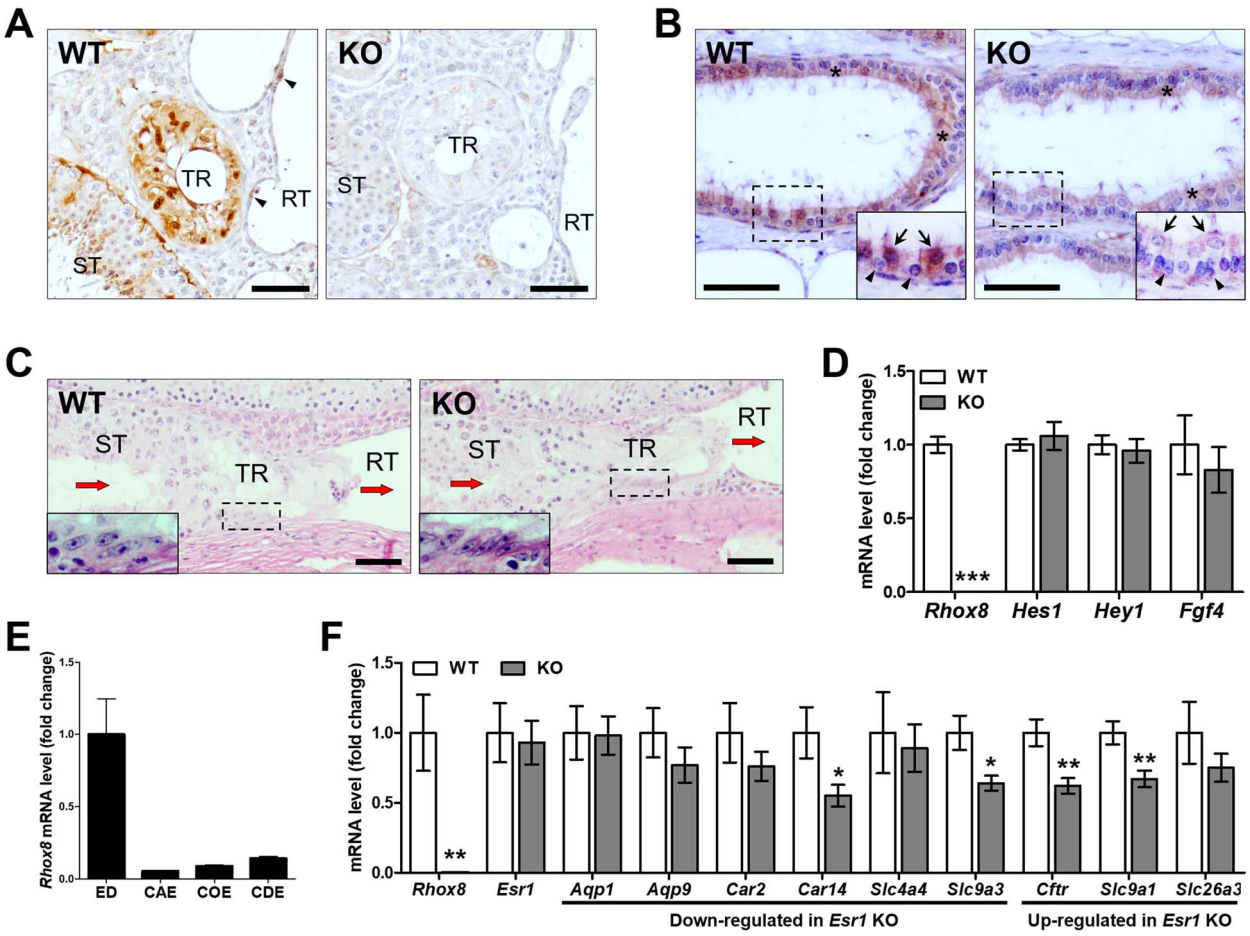

Figure 5. Analysis of TR and EDs in adult WT and *Rhox8* KO mice. (A) Immunohistochemical analysis for RHOX8 in the ST, TR, and RT. In the WT, the RHOX8 protein is localized to Sertoli cells in the ST and TR and to a few epithelial cells (arrowheads) in the RT, whereas it is not detectable in the *Rhox8* KO. Scale bars, 50 μm. (B) Immunohistochemical analysis for RHOX8 in the EDs. The RHOX8 protein is localized to ciliated cells (arrows) in WT EDs. Insets presents magnified images of the boxed regions. Arrowheads, non-ciliated cells. Asterisks indicate non-specific staining in the cytoplasm of epithelium. Scale bars, 50 μm. (C) Testis sections were stained with hematoxylin and eosin to show the morphology of the modified Sertoli cells in the TR. Both WT and KO show normal valve-like structured Sertoli cells. Insets presents magnified images of the boxed regions. Red arrows indicate the directions of luminal flow. Scale bars, 50 μm. (D) Quantitative RT-PCR analysis of Notch signaling pathway genes in WT and *Rhox8* KO testes ($n = 6$). (E) Quantitative RT-PCR analysis of *Rhox8* mRNA in WT EDs and epididymis ($n = 3$). CAE, caput epididymis; COE, corpus epididymis; CDE, cauda epididymis. (F) Quantitative RT-PCR analysis of *Esr1*-regulated genes in WT and Rhox8 KO ED ($n = 6$). As an internal control, *Rpl19* mRNA was used. The data are presented as the means ± SEM. $^{**}P < 0.01$, $^{***}P < 0.001$.

specific transcription factors, *Rhox5* and *Gata1*, was examined. The mRNA level of *Rhox5* and *Gata1* was significantly lower in *Rhox8* KO testes than WT testes at P12, but there were no differences between WT and *Rhox8* KO at P30 and afterward (Figure 6), suggesting that *Rhox8* has a role in gene regulation as it regulates the other transcription factors in the Sertoli cells in a temporal manner. In addition, taking into account that the partial inhibition of the spermatogenic cycle in *Rhox8* KO mice (Figure 3E) and that *Rhox5* mRNA is induced by P7 and peaked at P12 [10] and *Gata4* is a marker of mature Sertoli cells in the mouse [33], it is suggested that there might be a developmental delay of germ cells during the first wave of spermatogenesis and that the reduction of *Rhox5* and *Gata1* mRNA at P12 could reflect the delayed germ cell development.

Discussion

The *Rhox* gene cluster was initially identified by our group [9, 34] and others [7, 35]. In the mouse, and most *Rhox* genes are expressed in germ cells of the testis and are differentially regulated in spermatogonia and spermatocyte [11, 35–37], suggesting the roles of *Rhox* genes in germ cell development. Recent studies have revealed the roles of several *Rhox* genes expressed in germ cells: *Rhox6* has a role in the determination of the germ cell lineage [38], *Rhox10* is involved in spermatogonial stem cell establishment as it induces pro-spermatogonia differentiation [39], and *Rhox13* is required for germ cell development, particularly during the first wave of spermatogenesis [40]. Within the *Rhox* cluster, only *Rhox5* and *Rhox8* are expressed in postnatal Sertoli cells [10]. We previously reported that total ablation of *Rhox5* results in male subfertility together with increased germ cell apoptosis and decreased sperm concentration and motility [9]. In the embryonic/fetal gonads, only *Rhox8* is expressed in Sertoli cells, while *Rhox5* is expressed in germ cells [11], suggesting a potentially unique role of *Rhox8* in Sertoli cell specification, differentiation, and function during embryonic testis development. The goal of this study was to examine the impact of total ablation of *Rhox8* in Sertoli cells at all ages.

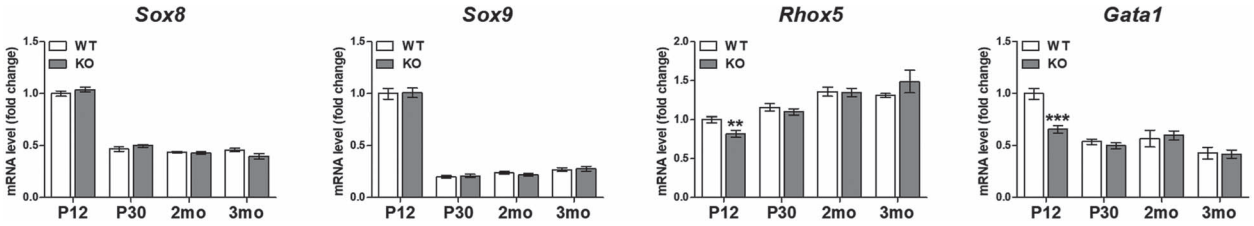

Figure 6. Analysis of gene expressions in the testes of WT and *Rhox8* KO mice. Quantitative RT-PCR analysis of *Sox8*, *Sox9*, *Rhox5*, and *Gata1* mRNA was performed using the testes at 12 days (P12), 30 days (P30), 2 months (2mo), and 3 months (3mo) of age. As an internal control, *Rpl19* mRNA was used. The data are presented as the means ± SEM ($n = 6$). $^{**}P < 0.01$, $^{***}P < 0.001$.

Characterization of our new *Rhox8*-null mouse revealed that *Rhox8* is required for optimal spermatogenesis and male fertility. *Rhox8* deletion elicited low male fecundity with disrupted spermatogenic cycles, increased germ cell apoptosis, and decreased sperm count and motility. These observations recapitulated and were only slightly more severe than the phenotype observed in the RHOX8 knockdown males [10]. However, interestingly, testis weights were increased by 14% in *Rhox8* KO mice, inconsistent with the phenotype of RHOX8 knockdown mice in which the testis mass was decreased by 16.5% [10]. This opposite result was also shown in ST diameter: the tubule diameter was increased in *Rhox8* KO, while RHOX8 knockdown showed the decreased tubule diameter. In addition, *Rhox8* KO showed a dilated RT, which has not been observed in the RHOX8 knockdown mice. We previously characterized the epididymal expression of the *Rhox* cluster and *Rhox8* is highly expressed in the rodent epididymis [9, 18]. Previously, no reduction in *Rhox8* mRNA and protein was observed in the epididymis of RHOX8 knockdown mice, presumably because the transgene did not produce a sufficient inhibitory response to impede translation [10]. As the mutant mice used in this study is a global KO, *Rhox8* was also deleted in the other reproductive tissues including epididymis. Thus, the increased testis size and dilated STs and RT in the *Rhox8* KO mice may be attributed to the ablation of *Rhox8* in the other excurrent ducts rather than a testis-specific defect. Indeed, in previous studies using global *Esr1* KO mouse, the *Esr1* KO testes at P35 to 3mo exhibited an increased testis size with disruption of spermatogenesis, dilated STs and RT, and reduced sperm counts and motility [29, 30, 41], which is similar to those of *Rhox8* KO explored in the present study. In the *Esr1* KO males, these phenotypes are related to dysfunction of EDs in which the fluid reabsorption from the lumen is inhibited by *Esr1* deletion [29]. In our analysis of the excurrent ducts, *Rhox8* mRNA in the EDs was relatively higher than that in caput, corpus, and cauda epididymis and RHOX8 protein was detected in the ciliated cells of the EDs. In addition, the expression of metabolism and transport related genes (*Car14*, *Slc9a3*, *Cftr*, and *Slc9a1*) were regulated by *Rhox8* ablation, but its regulation pattern was not coincident with that in *Esr1* KO. This suggests that RHOX8 in the EDs may have a role in maintaining normal testis morphology as it regulates the functional genes in the EDs through other than ESR1 pathway. In the ED epithelium, the ciliated cells serve to stir luminal fluids, and the non-ciliated cells are involved in fluid absorption [28]. Therefore, *Rhox8* might play a role via cross-talk between ciliated cells and non-ciliated cells. In addition, we speculate that *Rhox8* in the ciliated cells might have a role in propelling the luminal fluids toward the epididymis; hence, it is possible that loss of *Rhox8* in the EDs results in fluid reflux from the epididymis, contributing to the increased testis size.

The cycle of the seminiferous epithelium is defined by the association of germ cell types which are found within a cross section of an ST [24]. During a cycle of the seminiferous epithelium, the cycle is divided into 12 and 14 stages in the mouse and rat, respectively [25, 42]. It is important to identify the groups of genes that are expressed in each specific stage to understand their specific roles during germ cell development because Sertoli cell functions are regulated by the coordinated development of spermatogonia, spermatocytes, and spermatids and the potential consequences of the Sertoli–germ cell interactions [43, 44]. Actually, many studies have described the stage-specific gene expression patterns in the Sertoli cells [43]. Especially, using staged testicular tissues or purified testicular cells, high-throughput analyses, such as microarray and RNA-seq, have revealed the genes expressed in a stage-specific manner in the Sertoli cells of mice and rats [45, 46]. Previously, through immunostaining of RHOX8 on the mouse testes, we showed that RHOX8 is expressed in all the stages during the cycle of the seminiferous epithelium [10]. But, in that study, we could not investigate whether there is a specific pattern or difference in *Rhox8* expression in each stage. Recently, the Griswold lab has reported the stage-specific transcriptomes using the Sertoli cells isolated from the mouse testes in which spermatogenesis was synchronized after WIN18,446 and retinoic acid treatment [45, 47]. They showed that *Rhox8* expression increases from stage I to III, peaks at stage VII–VIII, and then, decreases until stage XI–XII [45]. In the present study, interestingly, the staging of the seminiferous epithelium in *Rhox8* KO mice showed an increase in STs at stage I–VI and a significant reduction at stage VII–VIII when the *Rhox8* expression is the highest during the cycling. Between stage VI and VII, type B spermatogonia differentiate into preleptotene spermatocytes [24], i.e., meiosis begins at this time point. Therefore, it is suggested that *Rhox8* regulates the genes involved in meiosis during spermatogenesis. In addition, at stage IX–XII, there were no significant differences between WT and *Rhox8* KO, indicating a normal spermatogenesis during this period, which implies a crucial role of *Rhox8* at the stage VII–VIII rather than at the later stages including spermiation. Taking into account that the action of retinoic acid is required for spermatogonial differentiation and that the level of retinoic acid is high at stage VII–VIII when type A spermatogonia differentiate into type A1 spermatogonia [48, 49], the highest level of *Rhox8* expression at stage VII and VIII implies a possible role of *Rhox8* in retinoic acid signaling pathway during spermatogonia differentiation.

We have previously reported that *Rhox5* ablation results in the misregulation of the majority of the *Rhox* gene cluster including *Rhox8* in the epididymis [18] and that *Rhox8* expression is dependent upon RHOX5 during early folliculogenesis in the ovary [19], suggesting that *Rhox8* expression is regulated by *Rhox5* in the epididymis and ovary. However, our lab and others have not been able to identify changes in *Rhox* gene expression in the testes of *Rhox5*-null mice in previously published and unpublished works. Herein, quantitative RT-PCR showed that the expression of *Rhox5* mRNA is reduced by *Rhox8* ablation in the testes at P12, suggesting that *Rhox8* regulates *Rhox5* in the testis, which implies tissue-specific differences in the cross-regulation of genes within the *Rhox* cluster. In addition to the downregulation of *Rhox5*, *Gata1*, a marker of mature Sertoli cells [33], was also downregulated by *Rhox8* ablation at P12. The regulation of the other transcription factors by *Rhox8* suggest that *Rhox8* controls the gene network in the testis as it plays upstream of the other regulators during testis development. To reveal the molecular mechanism by which RHOX8 controls the gene network in the testis, an integrated analysis of transcriptome and cistrome through RNA-seq and ChIP-seq using *Rhox8* KO model should be performed in the future. Subsequently, the expression of *Rhox5* and *Gata1* was not different between WT and *Rhox8* KO testes from P30 to 3mo. Regarding this, there is a notion that must be considered to interpret the gene expressions produced from whole testis tissues. In mice, after birth, Sertoli cell proliferation continues until around P12 when the Sertoli cells show their typical adult appearance with a high proportion (39%) in the testis [22, 50], and then, the proportion of the Sertoli cells continuously decrease until adulthood [51], indicating a relatively lower population of Sertoli cells in the testis from prepuberty to adulthood. Moreover, a study that examined the transcriptomes from whole testes after ablation of germ cells or Sertoli cells has revealed 701 Sertoli-specific transcripts and 4302 germ cell–specific transcripts among total 25 255 transcripts expressed in the mouse testis [3], indicating that extensive transcripts are expressed in both Sertoli and germ cells, although it could not be ignored that there are some transcripts specific for the other cell types such as interstitial cells including Leydig cells. Furthermore, in case of some genes including *Rhox8*, they are expressed in a stage-specific manner, which can show smaller changes in their expression than they actually are. Taken together, these factors preclude the identification of gene expression profiles changed within the Sertoli cells when whole testis tissues are subjected. To address this issue, the use of spatial transcriptomic technology would be definitely beneficial, which allows visualization and quantitative analysis of the transcriptome with spatial resolution in individual tissue sections [52].

In our previous study using RHOX8 knockdown mice, the expression of *Sox8* and *Sox9*, crucial regulators of testis development and function [32], were downregulated in the mutant at P18 and P30 [10]. This suggested that complete ablation of RHOX8 during embryonic testis development might reveal a role in sex determination. Many studies have characterized the transcription factor cascade that acts in Sertoli cells to promote male development [53, 54]. In this study, the expression of the key genes for embryonic gonad development (*Sox9*, *Fgf9*, *Fgfr2*, *Ptgds*, *Amh*, and *Wnt4*) was not changed by *Rhox8* ablation in the testes from E12.5 to E15.5, although the expression of *Pou5f1* and *Ddx4* showed a transitory change. Therefore, it is suggested that *Rhox8* in the Sertoli cells does not have an essential role in sex determination and embryonic testis differentiation. However, it could not be excluded that *Rhox8* may have a role in regulating the genes that orchestrate optimal gonad development or that upregulation or compensation by other unexamined testis-promoting factors may occur to replace lost RHOX8. A further study that analyzes the transcriptomic change in the *Rhox8* KO would be helpful to determine whether and understand if *Rhox8* subtly contributes to gonad function during testis development.

At present, it is a mystery why *Sox* gene misregulation was not recapitulated in our new *Rhox8* KO mice. The knockdown model that we employed was developed by Manjeet Rao and Miles Wilkinson and was successful in the Sertoli-specific ablation of the tumor suppressor WT1 [16, 55]. This ablation resulted in germ cell death largely attributed to disruption of the blood–testis barrier. Consistent with that transgene becoming postnatally active via *Rhox5*'s Sertoli-specific androgen regulated promoter, no obvious differences in sex determination were observed and the expression of *Sox8* and *Sox9* was not examined in postnatal WT1-knockdown mice. Inhibitory siRNAs (typically 21 base pair hairpin structures) are an effective tool for specific gene silencing for experimental and therapeutic purposes in diverse tissues. Nevertheless, it could not be excluded that the siRNAs might affect the expression of off-target genes. Indeed, siRNAs can unexpectedly stimulate or repress the expression of non-specific genes in a concentration-dependent manner [56]. In addition, during the process of RNAi, DROSHA and DICER, RNase III family enzymes, have central roles in the biogenesis of miRNAs and siRNAs, which act targeting mRNAs for translational repression and degradation of endogenous genes [57]. In our knockdown mice, some of those factors could have been sequestered from their normal role in regulating genes such as *Sox9* due the need to process an excessive load siRNAs produced in RHOX8 knockdown Sertoli cells, which might cause systemic deregulation of genes in the Sertoli cells. This indirect effect may explain the disagreement between our prior and current RHOX8 mutant lines. Unfortunately, the RHOX8 siRNA knockdown mice are now defunct and it is impossible to elucidate whether there are non-specific gene regulation events and by which mechanism they occurred.

In summary, we generated a new mutant mouse model, *Rhox8* KO, using the CRISPR/Cas9 system to overcome the limits that a previous animal model retains and explored its phenotypes through a series of assessments including a breeding test, sperm analysis, apoptotic and histological evaluation, and gene expression analysis. The *Rhox8* KO showed normal sex determination and embryonic/fetal testis development, suggesting that *Rhox8* is dispensable for testis development during the embryonic development. However, *Rhox8* KO adult males showed disrupted spermatogenic cycle, increased germ cell apoptosis, and reduced sperm count and motility, resulting in male subfertility. In addition, these mice showed an enlarged testis accompanied with a dilated RT, which is a new finding that has not been observed in the previous mutant model. Collectively, *Rhox8* is required for complete testis development postnatally and optimal male fertility. Further investigations using high-throughput sequencing technologies such as RNA-seq and ChIP-seq are needed to understand the mechanism how *Rhox8*, as a regulator of the spermatogenesis, controls the gene network in the testis.

Acknowledgments

This work was substantially supported by grant R01HD093802 (James A. MacLeann II PI) from the National Institute of Health – Eunice Kennedy Shriver National Institute of Child Health & Human Development. We would like to thank Stacey McGee for sample embedding.

Supplementary data

Supplementary data are available at *BIOLRE* online.

Author contributions

YO, KH, and JAM designed research; YO, MK, JCD, and JAM performed research; CJB and NS assisted research techniques; YO, MK, KH, and JAM analyzed data; YO and JAM wrote the paper; all authors read and approved the manuscript.

Conflict of Interest

The authors have declared that no conflict of interest exists.

Data availability

The data underlying this article are available in the article and in its online supplementary material (Supplementary Table S1) and will be shared on reasonable request to the corresponding author.

References

1. Rato L, Alves MG, Socorro S, Duarte AI, Cavaco JE, Oliveira PF. Metabolic regulation is important for spermatogenesis. *Nat Rev Urol* 2012; **9**:330–338.
2. Maclean JA 2nd, Wilkinson MF. Gene regulation in spermatogenesis. *Curr Top Dev Biol* 2005; **71**:131–197.
3. Soffientini U, Rebourcet D, Abel MH, Lee S, Hamilton G, Fowler PA, Smith LB, O'Shaughnessy PJ. Identification of Sertoli cell-specific transcripts in the mouse testis and the role of FSH and androgen in the control of Sertoli cell activity. *BMC Genomics* 2017; **18**:972.
4. McGinnis W, Krumlauf R. Homeobox genes and axial patterning. *Cell* 1992; **68**:283–302.
5. Krumlauf R. Hox genes in vertebrate development. *Cell* 1994; **78**: 191–201.
6. Svingen T, Koopman P. Involvement of homeobox genes in mammalian sexual development. *Sex Dev* 2007; **1**:12–23.
7. MacLean JA 2nd, Wilkinson MF. The Rhox genes. *Reproduction* 2010; **140**:195–213.
8. MacLean JA 2nd. The role of Rhox homeobox factors in tumorigenesis. *Front Biosci (Landmark Ed)* 2013; **18**:474–492.
9. Maclean JA 2nd, Chen MA, Wayne CM, Bruce SR, Rao M, Meistrich ML, Macleod C, Wilkinson MF. Rhox: a new homeobox gene cluster. *Cell* 2005; **120**:369–382.
10. Welborn JP, Davis MG, Ebers SD, Stodden GR, Hayashi K, Cheatwood JL, Rao MK, MacLean JA 2nd. Rhox8 ablation in the Sertoli cells using a tissue-specific RNAi approach results in impaired male fertility in mice. *Biol Reprod* 2015; **93**:8.
11. Daggag H, Svingen T, Western PS, van den Bergen JA, McClive PJ, Harley VR, Koopman P, Sinclair AH. The rhox homeobox gene family shows sexually dimorphic and dynamic expression during mouse embryonic gonad development. *Biol Reprod* 2008; **79**:468–474.
12. Cong L, Ran FA, Cox D, Lin S, Barretto R, Habib N, Hsu PD, Wu X, Jiang W, Marraffini LA, Zhang F. Multiplex genome engineering using CRISPR/Cas systems. *Science* 2013; **339**:819–823.
13. Oh YS, Koh IK, Choi B, Gye MC. ESR1 inhibits hCG-induced steroidogenesis and proliferation of progenitor Leydig cells in mice. *Sci Rep* 2017; **7**:43459.
14. Barton BE, Rock JK, Willie AM, Harris EA, Finnerty RM, Herrera GG, Anamthathmakula P, Winuthayanon W. Serine protease inhibitor disrupts sperm motility leading to reduced fertility in female mice†. *Biol Reprod* 2020; **103**:400–410.
15. Shi M, Langholt EM, Butler LC, Harvey ME, Wheeler EC, Zhao L, MacLean JA, Oh Y, Sabrowsky E, Yu S, Watson S, Davis JF, *et al.* Vapor cannabis exposure generationally affects male reproductive functions in mice. *Toxicol Sci* 2022; **185**:128–142.
16. Rao MK, Pham J, Imam JS, MacLean JA, Murali D, Furuta Y, Sinha-Hikim AP, Wilkinson MF. Tissue-specific RNAi reveals that WT1 expression in nurse cells controls germ cell survival and spermatogenesis. *Genes Dev* 2006; **20**:147–152.
17. Salmon NA, Handyside AH, Joyce IM. Expression of Sox8, Sf1, Gata4, Wt1, Dax1, and Fog2 in the mouse ovarian follicle: implications for the regulation of Amh expression. *Mol Reprod Dev* 2005; **70**:271–277.
18. MacLean JA 2nd, Hayashi K, Turner TT, Wilkinson MF. The Rhox5 homeobox gene regulates the region-specific expression of its paralogs in the rodent epididymis. *Biol Reprod* 2012; **86**: 189.
19. Brown RM, Davis MG, Hayashi K, MacLean JA. Regulated expression of Rhox8 in the mouse ovary: evidence for the role of progesterone and RHOX5 in granulosa cells. *Biol Reprod* 2013; **88**:126.
20. Nah WH, Oh YS, Hwang JH, Gye MC. Changes in aquaporin 5 in the non-ciliated cells of mouse oviduct according to sexual maturation and oestrous cycle. *Reprod Fertil Dev* 2017; **29**:336–344.
21. Cao Y, Liu L, Lin J, Sun P, Guo K, Li S, Li X, Lan ZJ, Wang H, Lei Z. Dysregulation of notch-FGF signaling axis in germ cells results in cystic dilation of the rete testis in mice. *J Cell Commun Signal* 2022; **16**:75–92.
22. Bellvé AR, Cavicchia JC, Millette CF, O'Brien DA, Bhatnagar YM, Dym M. Spermatogenic cells of the prepuberal mouse. Isolation and morphological characterization. *J Cell Biol* 1977; **74**:68–85.
23. MacLean JA 2nd, Hu Z, Welborn JP, Song HW, Rao MK, Wayne CM, Wilkinson MF. The RHOX homeodomain proteins regulate the expression of insulin and other metabolic regulators in the testis. *J Biol Chem* 2013; **288**:34809–34825.
24. Russell LD, Ettlin RA, Sinha Hikim AP, Clegg ED. *Histological and Histopathological Evaluation of the Testis*. Clearwater, Florida: Cache River Press; 1990.
25. Oakberg EF. Duration of spermatogenesis in the mouse and timing of stages of the cycle of the seminiferous epithelium. *Am J Anat* 1956; **99**:507–516.
26. Ahmed EA, de Rooij DG. Staging of mouse seminiferous tubule cross-sections. *Methods Mol Biol* 2009; **558**:263–277.
27. Figueiredo AFA, Hess RA, Batlouni SR, Wnuk NT, Tavares AO, Abarikwu SO, Costa GMJ, Franca LR. Insights into differentiation and function of the transition region between the seminiferous tubule and rete testis. *Differentiation* 2021; **120**:36–47.
28. Hess RA. *Efferent Ductules: Structure and Function*, 2nd ed. Amsterdam, Netherlands: Elsevier Inc; 2018: 270–278.
29. Hess RA, Bunick D, Lee KH, Bahr J, Taylor JA, Korach KS, Lubahn DB. A role for oestrogens in the male reproductive system. *Nature* 1997; **390**:509–512.
30. Lee KH, Hess RA, Bahr JM, Lubahn DB, Taylor J, Bunick D. Estrogen receptor alpha has a functional role in the mouse rete testis and efferent ductules. *Biol Reprod* 2000; **63**:1873–1880.
31. Hess RA. Disruption of estrogen receptor signaling and similar pathways in the efferent ductules and initial segment of the epididymis. *Spermatogenesis* 2014; **4**:e979103.
32. Barrionuevo F, Scherer G. SOX E genes: SOX9 and SOX8 in mammalian testis development. *Int J Biochem Cell Biol* 2010; **42**: 433–436.
33. Viger RS, de Mattos K, Tremblay JJ. Insights into the roles of GATA factors in mammalian testis development and the control of fetal testis gene expression. *Front Endocrinol (Lausanne)* 2022; **13**:902198.
34. MacLean JA 2nd, Lorenzetti D, Hu Z, Salerno WJ, Miller J, Wilkinson MF. Rhox homeobox gene cluster: recent duplication of three family members. *Genesis* 2006; **44**:122–129.

35. Geyer CB, Eddy EM. Identification and characterization of Rhox13, a novel X-linked mouse homeobox gene. *Gene* 2008; **423**: 194–200.
36. Song HW, Dann CT, McCarrey JR, Meistrich ML, Cornwall GA, Wilkinson MF. Dynamic expression pattern and subcellular localization of the Rhox10 homeobox transcription factor during early germ cell development. *Reproduction* 2012; **143**:611–624.
37. Song HW, Anderson RA, Bayne RA, Gromoll J, Shimasaki S, Chang RJ, Parast MM, Laurent LC, de Rooij DG, Hsieh TC, Wilkinson MF. The RHOX homeobox gene cluster is selectively expressed in human oocytes and male germ cells. *Hum Reprod* 2013; **28**:1635–1646.
38. Liu C, Tsai P, García AM, Logeman B, Tanaka TS. A possible role of reproductive Homeobox 6 in primordial germ cell differentiation. *Int J Dev Biol* 2011; **55**:909–916.
39. Tan K, Song HW, Wilkinson MF. RHOX10 drives mouse spermatogonial stem cell establishment through a transcription factor signaling cascade. *Cell Rep* 2021; **36**:109423.
40. Busada JT, Velte EK, Serra N, Cook K, Niedenberger BA, Willis WD, Goulding EH, Eddy EM, Geyer CB. Rhox13 is required for a quantitatively normal first wave of spermatogenesis in mice. *Reproduction* 2016; **152**:379–388.
41. Eddy EM, Washburn TF, Bunch DO, Goulding EH, Gladen BC, Lubahn DB, Korach KS. Targeted disruption of the estrogen receptor gene in male mice causes alteration of spermatogenesis and infertility. *Endocrinology* 1996; **137**:4796–4805.
42. Leblond CP, Clermont Y. Definition of the stages of the cycle of the seminiferous epithelium in the rat. *Ann N Y Acad Sci* 1952; **55**:548–573.
43. Griswold MD. *Sertoli Cell Biology*. Amsterdam, Netherlands: Elsevier; 2015.
44. Griswold MD. 50 years of spermatogenesis: Sertoli cells and their interactions with germ cells. *Biol Reprod* 2018; **99**:87–100.
45. Gewiss RL, Law NC, Helsel AR, Shelden EA, Griswold MD. Two distinct Sertoli cell states are regulated via germ cell crosstalk†. *Biol Reprod* 2021; **105**:1591–1602.
46. Johnston DS, Wright WW, Dicandeloro P, Wilson E, Kopf GS, Jelinsky SA. Stage-specific gene expression is a fundamental characteristic of rat spermatogenic cells and Sertoli cells. *Proc Natl Acad Sci U S A* 2008; **105**:8315–8320.
47. Hogarth CA, Evanoff R, Mitchell D, Kent T, Small C, Amory JK, Griswold MD. Turning a spermatogenic wave into a tsunami: synchronizing murine spermatogenesis using WIN 18,446. *Biol Reprod* 2013; **88**:40.
48. Griswold MD. Spermatogenesis: the commitment to meiosis. *Physiol Rev* 2016; **96**:1–17.
49. Griswold MD. Cellular and molecular basis for the action of retinoic acid in spermatogenesis. *J Mol Endocrinol* 2022; **69**: T51–t57.
50. Vergouwen RP, Jacobs SG, Huiskamp R, Davids JA, de Rooij DG. Proliferative activity of gonocytes, Sertoli cells and interstitial cells during testicular development in mice. *J Reprod Fertil* 1991; **93**: 233–243.
51. Vergouwen RP, Huiskamp R, Bas RJ, Roepers-Gajadien HL, Davids JA, de Rooij DG. Postnatal development of testicular cell populations in mice. *J Reprod Fertil* 1993; **99**: 479–485.
52. Ståhl PL, Salmén F, Vickovic S, Lundmark A, Navarro JF, Magnusson J, Giacomello S, Asp M, Westholm JO, Huss M, Mollbrink A, Linnarsson S, *et al.* Visualization and analysis of gene expression in tissue sections by spatial transcriptomics. *Science* 2016; **353**: 78–82.
53. Vining B, Ming Z, Bagheri-Fam S, Harley V. Diverse regulation but conserved function: SOX9 in vertebrate sex determination. *Genes (Basel)* 2021; **12**:12.
54. Jiménez R, Burgos M, Barrionuevo FJ. Sex maintenance in mammals. *Genes (Basel)* 2021; **12**:12.
55. Rao MK, Wilkinson MF. Tissue-specific and cell type-specific RNA interference in vivo. *Nat Protoc* 2006; **1**:1494–1501.
56. Persengiev SP, Zhu X, Green MR. Nonspecific, concentration-dependent stimulation and repression of mammalian gene expression by small interfering RNAs (siRNAs). *RNA* 2004; **10**: 12–18.
57. Johanson TM, Lew AM, Chong MM. MicroRNA-independent roles of the RNase III enzymes Drosha and Dicer. *Open Biol* 2013; **3**:130144.